INTERNATIONAL JOURNAL OF AUTOMOTIVE AND MECHANICAL ENGINEERING (IJAME)
ISSN: 2229-8649 e-ISSN: 2180-1606
VOL. 19, ISSUE 1, 9606 – 9622
DOI: https://doi.org/10.15282/ijame.19.1.2022.22.0741

ORIGINAL ARTICLE

Dry and Wet Lubrication Analysis for Multi-Material Hip Assembly

Ravikant[1,*], V.K. Mittal[1], and V. Gupta[2]

[1]Department of Mechanical Engineering, NIT Kurukshetra, 136119, India
[2]Department of Mechanical Engineering, CDLSIET, Panniwala Mota, 125077, India

ABSTRACT – Hip joint repair/replacement is one of the most thriving orthopedic surgical procedures in the human body. The group of patients undergoing hip replacement considerably includes young and physically active persons with varying movements thus requiring longer product life and ease of maintenance. Perfect lubrication in hip assembly ensures a low wear rate and better product life. The present work focuses on dry and wet lubrication analysis of complete implant assembly instead of an individual part. The assembly consists of a stem, head, liner and cup, each made of different materials like a ceramic femoral head mounted over a metallic femoral stem with a polyethylene liner and a metallic acetabular cup. In this work, eight metal-materials are considered for stem/cup, three ceramic materials for the head and two polyethylene materials for the liner. The combinations of these materials are evaluated for various mechanical parameters. Dry (μ = 0.13) and wet (μ = 0.05) lubricating conditions between the liner and femoral head have been considered and their effects on the head, liner and cup have been evaluated for the optimization of Hip joint design. Fifty percent of re-surgery cases arise because of excessive wear out resulting in aseptic loosening of the femoral head and liner interface. Femoral head of size 28 mm diameter with 2 mm thick liner and 3 mm thick acetabular cup are modeled and are analyzed for axial pay load of 2.3 kN. The maximum von mises stress and total deformation for various material combinations of implant assembly have been compared to select the most suitable one for the arthroplasty implantation. The combination of CoCrMo – Ceramics – HXLPE – CoCrMo demonstrates minimum stress and deformation for all three parts i.e. femoral head, liner and acetabular cup under present loading and boundary conditions. ZTA is emerged as the preferred ceramic material for femoral head having a higher compressive strength.

ARTICLE HISTORY
Received: 2nd Sept 2021
Revised: 6th Dec 2021
Accepted: 10th Apr 2022

KEYWORDS
Coefficient of friction;
Lubrication;
Implant;
Friction;
Dry and wet friction

NOMENCLATURE

THA	Total Hip Arthroplasty	ZTA	Zirconia-Toughened Alumina
FEM	Finite Element Method	ASTM	American Society for Testing and Materials
THR	Total Hip Replacement	ISO	International Organization for Standards
COF	Coefficient of Friction	HXLPE	Highly cross link polyethylene
UHMWPE	Ultra-High Molecular Weight Polyethylene	CoP	Ceramic on Plastic

INTRODUCTION

The hip joint is one of the most important shock absorbing and weight-bearing structures in a human body channelizing a variety of movements like normal gait, running, climbing, and jumping. Excessive wear due to diseases, injuries or aging may require hip repair/replacement. Total Hip Arthroplasty (THA) is one of the most successful applications of biomaterials to alleviate pain and restore the functional mobility of the joints [1-3]. Major factors for limiting the service life of the Total Hip Replacement (THR) are deformation and wear that occurs between the articulating surfaces i.e. femoral head and polyethylene liner [4-5]. More than two million hip replacements per annum are performed worldwide and surely will increase swiftly in the next few years due to increment in the elderly population [3, 6]. Aseptic loosening is the most frequent reason for the revision of hip prosthesis [7]. While 30 % to 50 % of revisions are reported only due to cup loosening [8]. Metal debris released from prosthesis may cause local toxicity [9]. As per collected data on the total joint replacement surgery, it is estimated that, by the end of 2030, the number of hip and knee replacements will rise by 174% and 673% respectively as compared to the present rate [3].

As per the Canadian Joint Replacement Registry, the number of knee and hip replacements has increased by 21.5%. In the present scenario, there is an increment in several young and higher physically active personals who are undergoing hip surgery [10-11]. Higher activity level causes higher frictional moment and deformation which finally increase the risk of implant loosening [12-13]. Thus, a better prosthesis is now required which functions over 20 to 25 years without any revision [14-15]. Surgical techniques, physiology of synovial fluid and human activity level are some important factors that affect the survival rate of the prosthesis [16-18]. Excessive wear rate and debris are some of the major factors which lead to a revision of surgery [19-20]. According to the UK and Canadian national survey, the revision rate of the prosthesis

*CORRESPONDING AUTHOR | Ravikant | ravisharma.nitk@gmail.com

© The Authors 2022. Published by Penerbit UMP. This is an open access article under the CC BY license.

varies between 8-10 %, within an average lifespan of 15 years [14]. Wear and deformation are influenced largely by lubricating layer and coefficient of friction (COF) [21-22]. Scholes et al., (2000) [23] demonstrates that a thicker lubricating layer leads to lower friction coefficients. Hence, wear due to friction is the main measurable outcome for evaluating the performance of hip prosthesis. Preclinical testing is the standard procedure to predict the mechanical performance of the newly manufactured device. Wear test with multiple materials and designs had been performed [24].

The hip joint consists of a ball and socket joint with conformal contact. Prosthesis femoral head size is an essential criterion for the joint [25-26,64]. As per the ISO standard 28 mm, 32mm and 36 mm diameter femoral heads are generally used for the prosthesis, from which 28 mm diameter femoral head is most widely used [27]. While 36 mm metal to metal contact is termed as lowering wear and increasing stability [23, 26]. The coefficient of friction between the alumina-UHMWPE interface strongly depends upon the lubricant properties [28]. Lubricants like distal water (0.044), bovine serum (0.054) and saline (0.089) shows different friction coefficients, and increased up to 0.14 value i.e. non-lubrication (dry) condition [29]. Furthermore, some of the prominent work on hip prosthesis using finite element analysis is described in [68-74, 79]

In the present work, hip implant assembly with 28 mm diameter femoral head with three different materials and liner with two different materials have been considered with a variety of stem and cup materials. The boundary condition is taken as per the ISO standard with dry and wet conditions. The wet condition occurs due to the secretion of synovial fluid and the dry condition occurs when the secretion of lubricant from the body is limited. Dry condition is achieved when the body grows old and is unable to secret the physiological lubricating oil. Sobocinski [30] reveals that lower friction is obtained in Ceramic on Plastic combination. The present work also compares the mechanical behavior of femoral head with three standard commercially available ceramic materials, namely alumina, zirconia and zirconia-toughened alumina (ZTA), articulate against plastic liner material i.e. ultra-high molecular weight polyethylene (UHMWPE) and highly cross-link polyethylene (HXLPE). The FEM modeling of Charnley's hip implant having a 28 mm femoral head with a polyethylene liner and metallic cup has been developed using ANSYS. The results of stress and deformation are analyzed under static boundary conditions. Minimization of implant loosening has been a major concern, thus, effects of friction coefficient for head, liner and cup have been studied exclusively. The boundary conditions for the femoral stem have been considered as per American Society for Testing and Materials (ASTM) standards.

MATERIALS AND METHOD

Materials

The hip prosthesis is specifically made up of different materials like metal, ceramic, and plastics which have been studied exhaustively for specific roles as per their material properties and requirements, like ceramics with excellent compressive strength have been used for the femoral head. Similarly, metals are suitable for femoral stem and plastics for liner. UHMWPE is the traditional plastic material extensively used for hip liner replacement. After improving the drawbacks of UHMWPE, research lead to developing new material, named highly cross-link polyethylene (HXLPE) [31-32,75]. The first generation HXLPE (1998) is obtained by melting or annealing, while the second generation HXLPE (2005) is obtained by two different processes i.e. sequential repetition of irradiation and annealing cycles. The clinical outcomes of the second generation HXLPE ensured a reduction of wear up to 80% as compared to UHMWPE [33-34, 65-66].

The two widely used alloying metals in the designing of hip implant consist of titanium and CoCr alloys, which is achieved through cast and wrought processes. In the given material, the carbon content less than 0.15% plays a vital role in wear resistance. Assuming the material to be homogeneous, only linear compressive load is applied, effect of muscle and tissue contact have been neglected while applying the ASTM boundary conditions and wear between head and liner is not considered.

Materials like alumina, zirconia and ZTA are generally used as a high compressive bearing surface. ZTA is a relatively newcomer in the field of biomechanics. The revision rate of ceramic on plastic (CoP) combination is the lowest i.e. less than 2 % as compared to other combinations [21,76-78]. Materials like metals, ceramics and plastics with their main characteristics are given in Table 1 and Table 2. The coefficient of friction (COF) in Hip implant depends largely upon geometrical properties like the type of lubricant, and static/dynamic loading conditions. Clinical and experimental studies demonstrate the variation of friction coefficient while changing the material combination. Table 3 summarizes the typical values of COF under different material combinations.

Table 1. Material properties of femoral head and liner material [35-37].

Material type	Density (Kg/m^3)	Modulus (GPa)	Poisson's ratio	Ultimate strength (MPa)	Yield strength (MPa)
Alumina	3980	380	0.33	551	-
Zirconia	6040	110	0.30	330	230
ZTA	4380	358	0.23	350	290
UHMWPE (Liner)	930	0.690	0.43	40	21
HXLPE (Liner)	930	2.7	0.3	56.7	26.2

Table 2. Material properties of femoral stem and acetabular cup materials [38-40].

Material(s)	Density (Kg/m^3)	Modulus (GPa)	Poisson's ratio	Ultimate strength (MPa)	Yield strength (MPa)
Co-Cr-Mo (Cast)	8300	230	0.29	970	612
Ni-Ta Alloys	6450	83	0.3	895	690
Ti–6Al–4V	4500	110	0.32	900	800
Ti-6Al-7Nb	4510	120	0.33	1050	950
Ti-15Mo-5Zr	5060	78	0.33	960	920
Ti-15Mo-5Zr-3Al	4950	82	0.3	1475	900
Ti-13Nb-13Zr	4990	84	0.3	1037	900
Ti-29Nb-13Ta-4.6Zr	5000	80	0.3	911	864

Table 3. Coefficient of friction for different material combinations [30].

Material(s)	COF (Max.)	COF (Min.)
Ceramic on plastic	0.137	0.083
Metal on plastic	0.15/0.16	0.069/0.064
Ceramic on ceramic	0.43	0.30
Metal on metal	0.62	0.30

FEM Modeling

The finite element method is widely used in many areas of biomechanics and biomedical engineering. The numeric tool of the FEM has been widely used to study the behavior of joints and bones under tensile and compressive stresses. Charnley's implant is the most extensively accepted hip implant in the last four decades. The present model consists of four major parts named as a femoral stem, femoral head, liner and acetabular cup. The generated 3D-model of implant is depicted in Figure 1. Materials are assumed to be homogeneous and isotropic for each part. Most of the implant model available in previous studies considered smooth surfaces for the ease of solution. The present analysis is carried out for understanding the stress and deformation behavior for dry and wet conditions respectively. The value of friction coefficient for dry and wet conditions has been extracted from clinical and experimental studies on the hip implants [42-43].

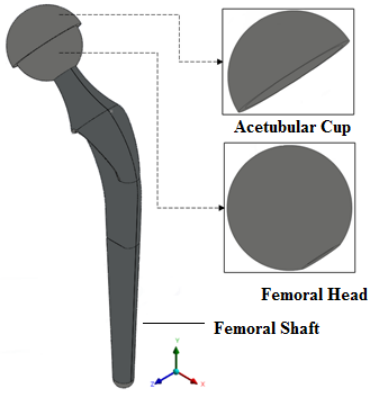

Figure 1. 3D CAD model of hip implant assembly.

Meshing

The mesh of the 3D model implant has been generated using tetrahedral elements. The meshed model contains 1304695 and 917535 number of nodes and elements respectively. These elements consist of three degrees of freedom at each nodal point i.e. translation in x, y and z directions and a quadratic behavior which is well suited for the meshing of highly complex curved geometries.

As the size of the elements decreases, the number of the elements increases proportionally. Increment in the number of the elements in the study continuously changes the values of stress and other mechanical parameters, which also takes larger time to solve the discretized problems. So, it becomes very difficult to clarify the size and the number of the elements suitable for the analysis. That is why grid independence test has been carried out for getting the optimum size and the number of the elements.

Figure3 illustrates mesh independence for the present implant. This figure clearly reflects the relation between the element numbers to the von- mises stress. It can be seen that the value of stress is changing up to 380000 elements, and beyond that, there is no major change occurring in von-mises stress. Thus, the 0.71 mm mesh size has been adopted for analyzing the present model.

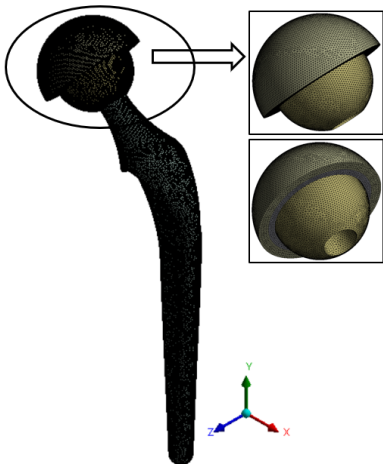

Figure 2. Meshed model of hip implant assembly.

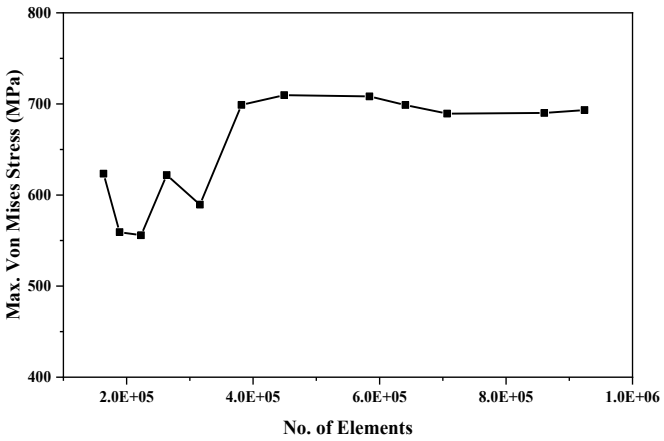

Figure 3. Grid independent test.

Boundary Conditions

The boundary conditions have been applied as per the ASTM F2996-13 and ISO 7206–4:2010(E) standards [45]. Torsional, rotating, tension and dynamic forces have not been taken into account due to the application of static liner loading. Frictional contact is considered into a contact surface between the femoral head and liner. All the material combinations have been analyzed for the 2.3 kN (approximately 3.5 times of standard bodyweight) static uniform compression loading applied over the metallic acetabular cup. The areas of the distal end are fixed in the present model as depicted in Figure 4.

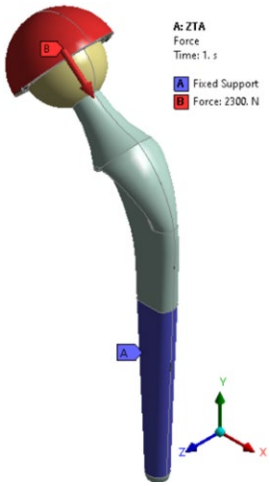

Figure 4. Boundary conditions,

FEA RESULTS

The simulation has been carried out for Charnley's implant to obtain the least deformation material-combination for dry and wet lubricating conditions. The present section compares the results obtained by considering eight different femoral stem materials, with alumina, zirconia and ZTA femoral head articulating against UHMWPE and HXLPE liner with the same metallic acetabular cup as the stem. Analytical results of finite element analysis of hip implant under a uniform static load of 2.3 kN have been depicted in Figure 5 and Figure 6. These two figures demonstrate analytical results for hip implant under dry ($\mu = 0.13$) and wet ($\mu = 0.05$) conditions with a material combination of Ti-6Al-7Nb – ZTA – UHMWPE – Ti-6Al-7Nb with the optimum limit of a factor of safety. The results of Von-mises stresses deformations and strains for head, liner and cup have been evaluated for the selection of suitable material combination for arthroplasty.

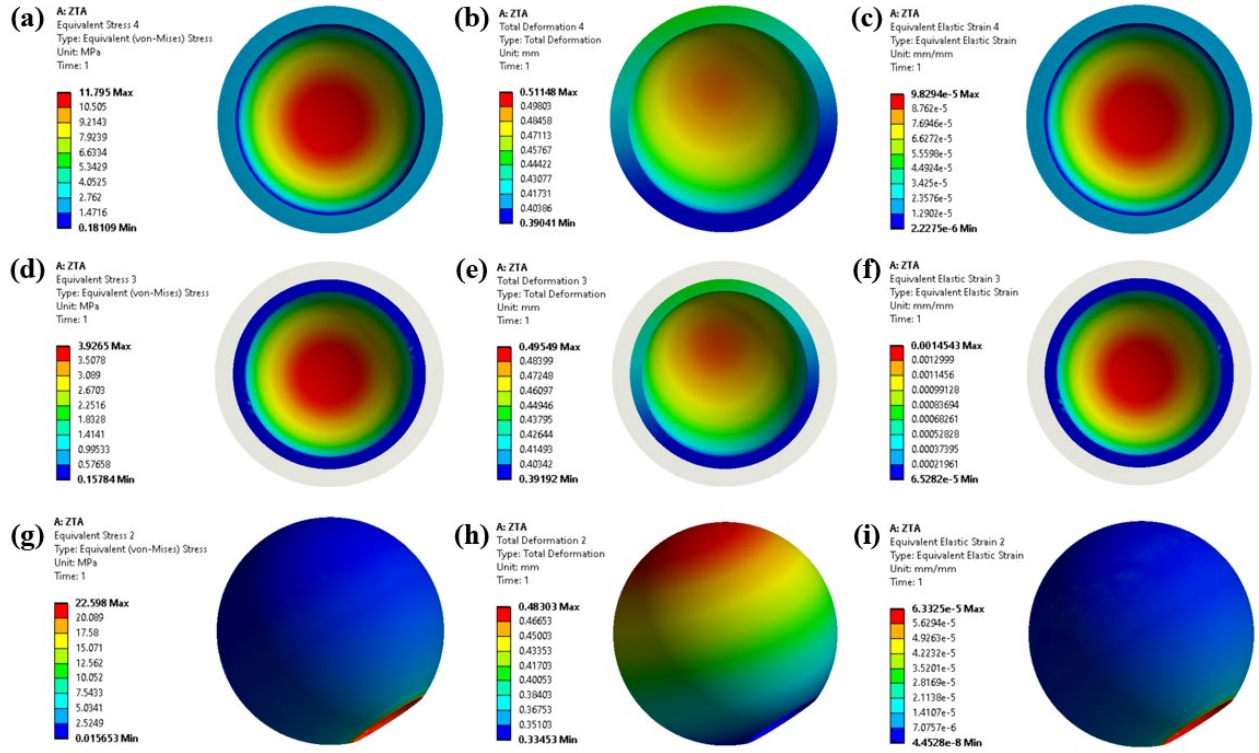

Figure 5. Contours of Ti-6Al-7Nb-ZTA-HXLPE-Ti-6Al-7Nb combination for dry lubricating condition (μ=0.13): (a) acetabular cup von-mises stress; (b) acetabular cup deformation; (c) acetabular cup strain; (d) liner von-mises stress; (e) liner deformation; (f) liner strain; (g) femoral head von-mises stress; (h) femoral head deformation; (i) femoral head strain.

As discussed earlier three different femoral head materials with two liner material have been considered (see Table 1) and the effect of friction coefficients have also been evaluated. Mechanical parameters like stress, deformation and strain of femoral head, liner and acetabular cup with dry lubricating conditions are depicted in Figure 5. In which, Figure 5(a), 5(b), and 5(c) illustrates stress, deformation and strain for HXLPE liner whereas, Figure 5(d), 5(e), 5(f) and 5(g), 5(h), 5(i) expresses stress, deformation and strain for Ti-6Al-7Nb acetabular cup and ZTA femoral head respectively. Similarly, for a wet lubricating condition, stress, deformation and strain for liner, acetabular cup and femoral head with the same material are depicted in Figure 6(a)-6(c), 6(d)-6(f) and 6(g)-6(i) respectively.

Stress and strain are maximum at the core of the liner and acetabular cup as depicted in Figure 5(a), 5(c) and 5(d), 5(f) and reduced towards the outermost radius under dry lubricating condition. Similarly, the femoral head demonstrates maximum concentration of stress and strain in the neck joint area. However, the maximum deformation for the liner-acetabular cup occurs at the medial side. The stress concentration and strain in acetabular cup are higher than liner. The similar contours have been obtained for wet lubricating condition as depicted in Figure 6 (a) to 6(i). After analyzing all possible combinations of these materials, it has been observed that the stress and deformation follow almost the same pattern for every material combination due to similar material properties under the same boundary and loading constraints.

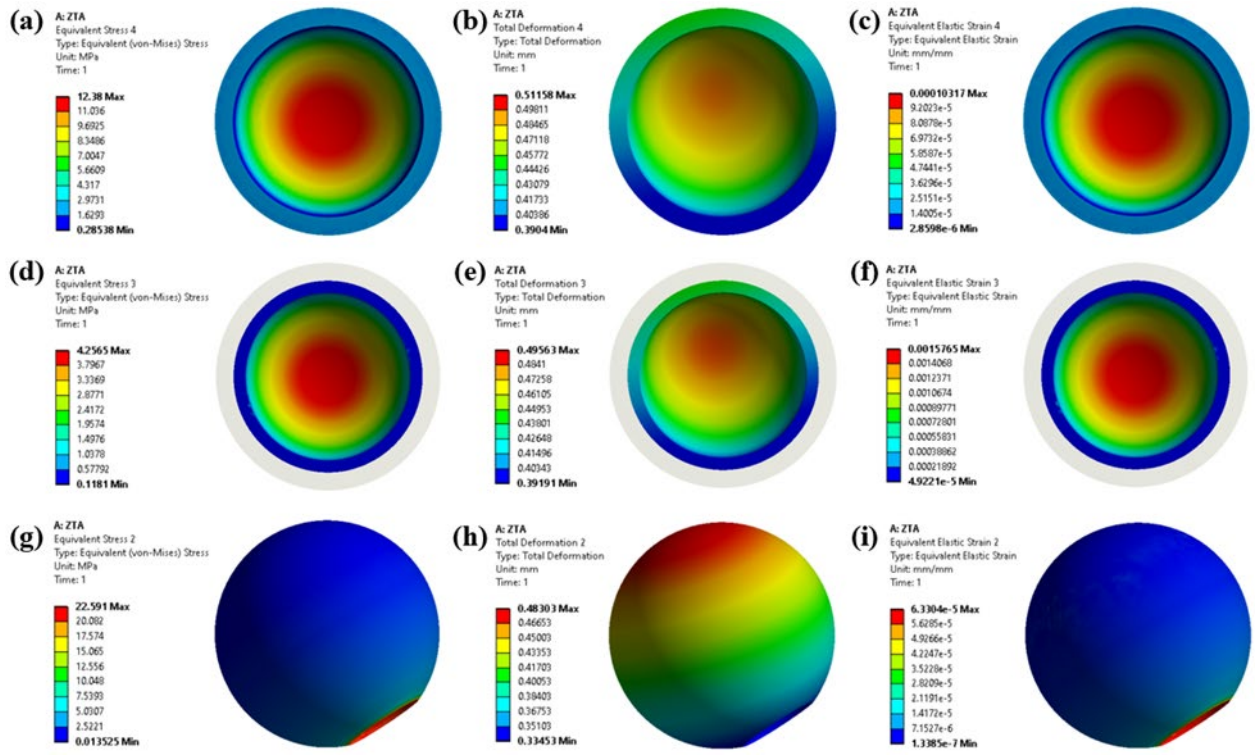

Figure 6. Contours of Ti-6Al-7Nb-ZTA-HXLPE-Ti-6Al-7Nb Combination for wet lubricating condition (μ=0.05): (a) acetabular cup von-mises stress; (b) acetabular cup deformation; (c) acetabular cup strain; (d) liner von-mises stress; (e) liner deformation; (f) liner strain; (g) femoral head von-mises stress; (h) femoral head deformation; (i) femoral head strain.

Stress Variation Analysis

The variation of stresses for liner, cup and head are depicted in Figure 7. Stress variation at the interior and exterior surfaces of the liner, cup and head under dry-wet lubrication from medial to the lateral side are depicted in Figure 7(a), 7(b) and 7(c) respectively. Wet lubrication demonstrates a greater value of stress as compared to dry condition. In liner, the exterior side demonstrates higher stress but for acetabular cup interior side showcase the maximum stress. The peak stress is observed at the center of the liner and cup and in the case of femoral head it is maximum towards the circumference as depicted in Figure 7(c).

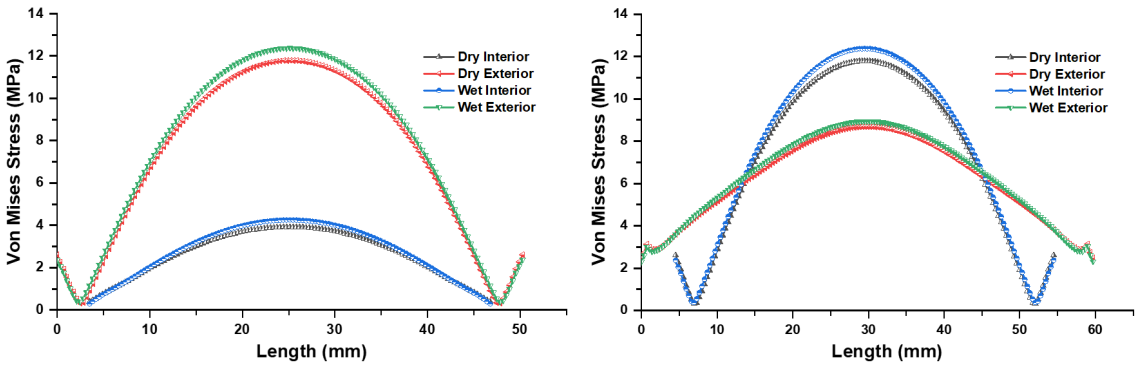

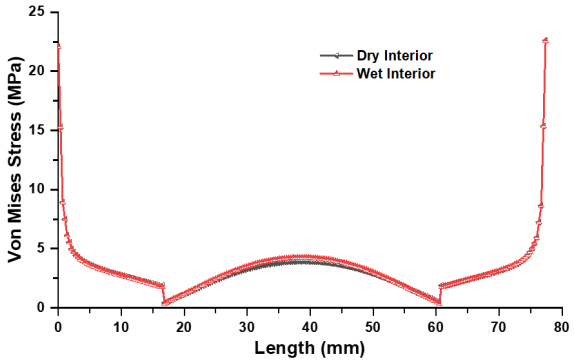

(c)

Figure 7. Variation of stress under dry and wet lubricating conditions: (a) liner; (b) acetabular cup and (c) femoral head.

Deformation Variation Analysis

Figure 8 depicts the variation of deformation on interior and exterior surface under dry-wet lubrication conditions. It is observed that there is not any significant difference in deformation at interior and exterior surfaces for liner and cup as shown in Figure 8(a) and 8(b) respectively. Dry lubrication leads to higher deformation, which increases from the medial side and reaches maximum at the centre and then continue to reduce towards the lateral end. Similar graph patterns have been obtained for liner, acetabular cup and femoral head, as depicted in Figure 8 (a), 8(b) and 8(c) respectively.

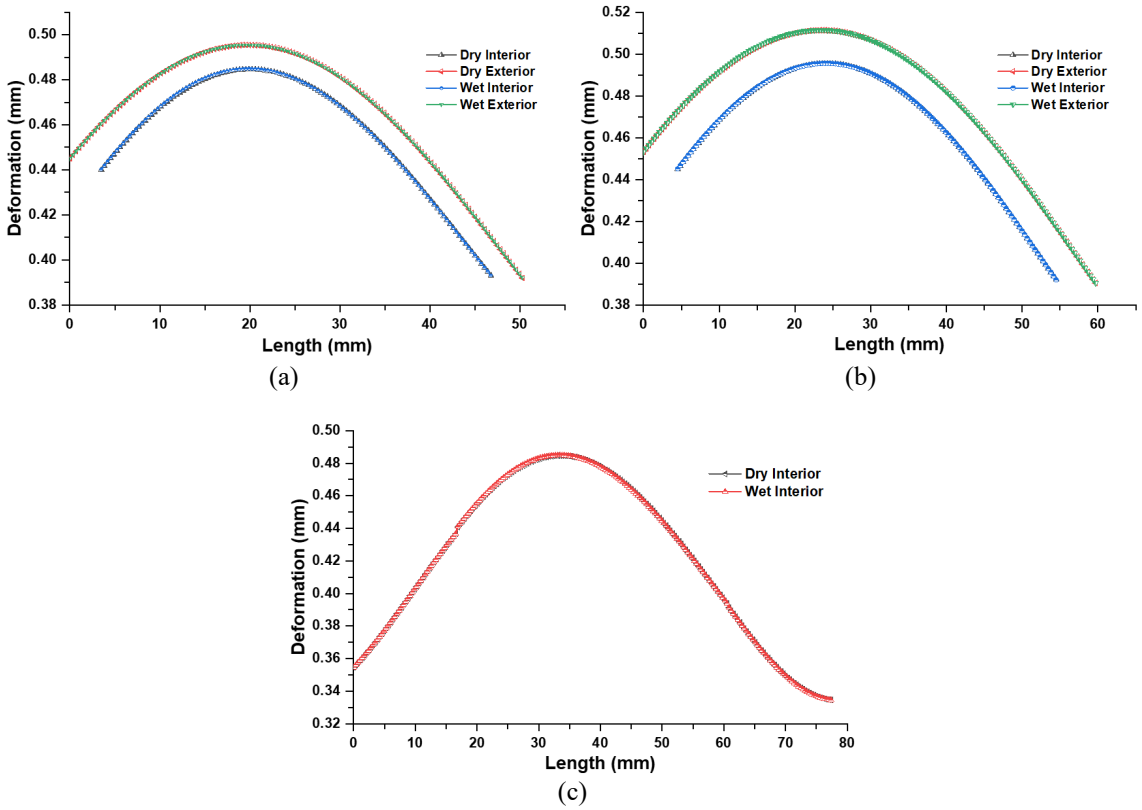

(a) (b)

(c)

Figure 8. Variation of deformation under dry and wet lubricating conditions: (a) liner; (b) acetabular cup and (c) femoral head.

Strain Variation Analysis

Figure 9 demonstrates strain variation under dry-wet lubrication conditions for interior and exterior faces. It is observed that the interior side of the liner under wet condition showcases the maximum strain followed by dry condition as shown in Figure 9(a). Strain difference between interior and exterior surfaces was greater in liner as shown in Figure 9(a) than acetabular cup which is shown in Figure 7(b). Strain for acetabular cup follows the same pattern as liner i.e. maximum strain occurred at interior surface under wet condition followed by dry lubrication. At the center of the femoral head, maximum stress is observed under wet conditions as shown in Figure 9(c). The strain starts increasing from the medial side and reaches to its maximum value at the center and then continue decreasing towards the lateral side.

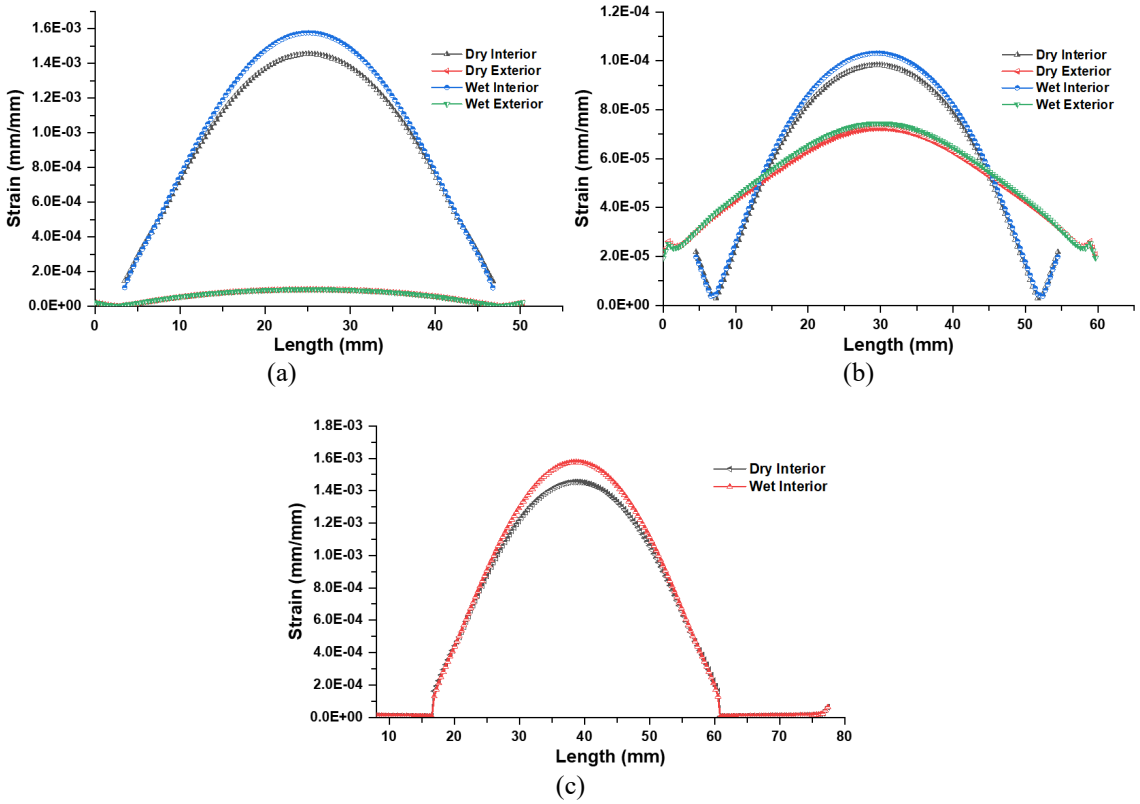

Figure 9. Variation of strain under dry and wet lubricating conditions: (a) liner; (b) acetabular cup and (c) femoral head.

Figure 10 illustrates the variation of stress for liner and acetabular cup under dry-wet lubrication at interior and exterior faces. Maximum stress is observed on interior side of acetabular cup under dry condition followed by wet condition. However, minimum stress occurs on the interior side of the liner. Stress patterns at the exterior side of liner were similar to the acetabular interior faces due to similar geometry.

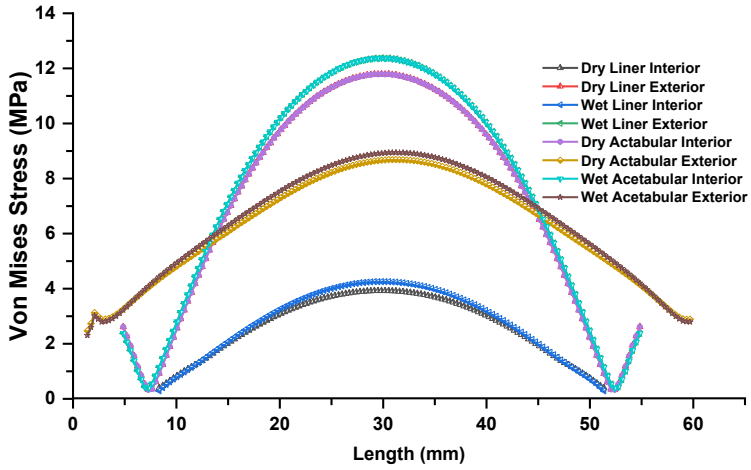

Figure 10. Variation of strain under dry and wet lubricating conditions for liner and acetabular cup.

The results obtained under 2.3kN static loading condition, for every possible material combination of (stem – head – liner – acetabular cup), are tabulated in Table 4 to Table 19. Mechanical parameters of material combinations like CoCrMo – Ceramics – HXLPE – CoCrMo for dry and wet conditions are summed up in Table 4. Similarly, Table 5 displays results obtained for UHMWPE liner material with a similar material configuration as in Table 4. Maximum von-mises stress is found in femoral head which reduces ascendingly towards acetabular cup and liner while maximum deformation follows ascending order of acetabular cup, liner and femoral head.

Von-mises stress and deformation of HXLPE and UHMWPE with femoral stem and liner material are tabulated in Table 4-19. Mechanical parameter for HXLPE and UHMWPE liner material have been demonstrated for combination CoCrMo (Table 4 and 5), Ti-6Al-7Nb (Table 6 and 7), Ti-6Al-4V (Table 8 and 9), Ti-29Nb-13Ta-4.6Zr (Table 10 and 11), Ti-13Nb-13Zr (Table 12 and 13), Ni-Ta (Table 14 and 15), Ti-15Mo-5Zr-3Al (Table 16 and 17), Ti-15Mo-5Zr (Table 18 and 19) respectively.

Table 4. Mechanical parameters under static analysis of hip implant at dry and wet lubricating conditions with the combination of CoCrMo – ceramics – HXLPE – CoCrMo.

Ceramic		Femoral head		Liner		Acetabular cup	
		Stress (MPa)	Deformation (mm)	Stress (MPa)	Deformation (mm)	Stress (MPa)	Deformation (mm)
Alumina	Dry	20.559	0.25349	3.8716	0.26081	12.007	0.2692
	Wet	20.539	0.25349	4.1711	0.26093	12.549	0.26928
Zirconia	Dry	14.62	0.2537	3.8171	0.26105	11.923	0.26944
	Wet	14.577	0.25369	4.1207	0.26117	12.475	0.26952
ZTA	Dry	21.502	0.25349	3.8709	0.26082	12.007	0.26921
	Wet	21.48	0.25349	4.1718	0.26094	12.551	0.26929

Table 5. Mechanical parameters under static analysis of hip implant at dry and wet lubricating conditions with the combination of CoCrMo – ceramics – UHMWPE – CoCrMo.

Ceramic		Femoral head		Liner		Acetabular cup	
		Stress (MPa)	Deformation (mm)	Stress (MPa)	Deformation (mm)	Stress (MPa)	Deformation (mm)
Alumina	Dry	20.575	0.2535	1.8886	0.26437	12.889	0.27263
	Wet	20.546	0.25349	2.145	0.26485	13.741	0.273
Zirconia	Dry	14.635	0.25371	1.8828	0.26463	12.851	0.2729
	Wet	14.579	0.2537	2.132	0.26513	13.709	0.27328
ZTA	Dry	21.52	0.25349	1.8894	0.26438	12.889	0.27264
	Wet	21.489	0.25349	2.145	0.26487	13.743	0.27301

Table 6. Mechanical parameters under static analysis of hip implant at dry and wet lubricating condition with the combination of Ti-6Al-7Nb – Ceramics – HXLPE – Ti-6Al-7Nb.

Ceramic		Femoral head		Liner		Acetabular cup	
		Stress (MPa)	Deformation (mm)	Stress (MPa)	Deformation (mm)	Stress (MPa)	Deformation (mm)
Alumina	Dry	21.507	0.48304	3.9279	0.49548	11.796	0.51147
	Wet	21.499	0.48303	4.2565	0.49561	12.379	0.51157
Zirconia	Dry	20.521	0.48323	3.8783	0.49571	11.721	0.5117
	Wet	20.488	0.48322	4.2104	0.49585	12.313	0.51179
ZTA	Dry	22.59	0.48303	3.9265	0.49549	11.795	0.51148
	Wet	22.591	0.48303	4.2565	0.49563	12.38	0.51158

Table 7. Mechanical parameters under static analysis of hip implant at dry and wet lubricating condition with the combination of Ti-6Al-7Nb – Ceramics – UHMWPE – Ti-6Al-7Nb.

Ceramic		Femoral head		Liner		Acetabular cup	
		Stress (MPa)	Deformation (mm)	Stress (MPa)	Deformation (mm)	Stress (MPa)	Deformation (mm)
Alumina	Dry	21.517	0.48304	1.9145	0.4988	12.719	0.51474
	Wet	21.505	0.48304	2.1687	0.49927	13.624	0.5151
Zirconia	Dry	20.537	0.48324	1.9081	0.49904	12.687	0.51498
	Wet	20.494	0.48323	2.1566	0.49952	13.594	0.51535
ZTA	Dry	22.61	0.48304	1.9158	0.49881	12.72	0.51475
	Wet	22.598	0.48303	2.1687	0.49928	13.625	0.51511

Table 8. Mechanical parameters under static analysis of hip implant at dry and wet lubricating condition with the combination of Ti-6Al-4V – Ceramics – HXLPE – Ti-6Al-4V.

Ceramic		Femoral head		Liner		Acetabular cup	
		Stress (MPa)	Deformation (mm)	Stress (MPa)	Deformation (mm)	Stress (MPa)	Deformation (mm)
Alumina	Dry	21.663	0.52774	3.9403	0.54119	11.772	0.55866
	Wet	21.672	0.52774	4.2745	0.54133	12.359	0.55876
Zirconia	Dry	20.976	0.52793	3.8919	0.54142	11.696	0.55888
	Wet	20.944	0.52792	4.2295	0.54156	12.293	0.55898
ZTA	Dry	22.129	0.52774	3.9389	0.5412	11.771	0.55868
	Wet	22.122	0.52774	4.2745	0.54134	12.36	0.55877

Table 9. Mechanical parameters under static analysis of hip implant at dry and wet lubricating condition with the combination of Ti-6Al-4V – Ceramics – UHMWPE – Ti-6Al-4V.

Ceramic		Femoral head		Liner		Acetabular cup	
		Stress (MPa)	Deformation (mm)	Stress (MPa)	Deformation (mm)	Stress (MPa)	Deformation (mm)
Alumina	Dry	21.657	0.52775	1.92	0.54449	12.722	0.56192
	Wet	21.668	0.52774	2.174	0.54496	13.624	0.56228
Zirconia	Dry	20.992	0.52795	1.914	0.54472	12.689	0.56215
	Wet	20.951	0.52793	2.1622	0.5452	13.594	0.56252
ZTA	Dry	22.14	0.52774	1.9216	0.5445	12.722	0.56193
	Wet	22.129	0.52774	2.174	0.54497	13.626	0.56229

Table 10. Mechanical parameters under static analysis of hip implant at dry and wet lubricating condition with the combination of Ti-29Nb-13Ta-4.6Zr – Ceramics – HXLPE – Ti-29Nb-13Ta-4.6Zr.

Ceramic		Femoral head		Liner		Acetabular cup	
		Stress (MPa)	Deformation (mm)	Stress (MPa)	Deformation (mm)	Stress (MPa)	Deformation (mm)
Alumina	Dry	21.663	0.52774	3.9403	0.54119	11.772	0.55866
	Wet	22.43	0.72767	4.3529	0.74576	12.261	0.76981
Zirconia	Dry	20.976	0.52793	3.8919	0.54142	11.696	0.55888
	Wet	20.988	0.72786	4.3121	0.746	12.196	0.77004
ZTA	Dry	22.129	0.52774	3.9389	0.5412	11.771	0.55868
	Wet	22.81	0.72767	4.3527	0.74577	12.262	0.76982

Table 11. Mechanical parameters under static analysis of hip implant at dry and wet lubricating condition with the combination of Ti-29Nb-13Ta-4.6Zr – Ceramics – UHMWPE – Ti-29Nb-13Ta-4.6Zr.

Ceramic		Femoral head		Liner		Acetabular cup	
		Stress (MPa)	Deformation (mm)	Stress (MPa)	Deformation (mm)	Stress (MPa)	Deformation (mm)
Alumina	Dry	22.41	0.72768	1.9463	0.74885	12.687	0.77293
	Wet	22.425	0.72767	2.1978	0.74933	13.596	0.7733
Zirconia	Dry	21.028	0.72788	1.9398	0.74909	12.653	0.77316
	Wet	20.995	0.72787	2.1866	0.74958	13.566	0.77354
ZTA	Dry	22.787	0.72767	1.9469	0.74886	12.687	0.77294
	Wet	22.805	0.72767	2.1977	0.74934	13.597	0.77331

Table 12. Mechanical parameters under static analysis of hip implant at dry and wet lubricating condition with the combination of Ti-13Nb-13Zr – Ceramics – HXLPE – Ti-13Nb-13Zr.

Ceramic		Femoral head		Liner		Acetabular cup	
		Stress (MPa)	Deformation (mm)	Stress (MPa)	Deformation (mm)	Stress (MPa)	Deformation (mm)
Alumina	Dry	22.299	0.69302	3.9854	0.71019	11.674	0.73313
	Wet	22.31	0.69302	4.3398	0.71033	12.28	0.73324
Zirconia	Dry	20.999	0.69322	3.9407	0.71042	11.599	0.73336
	Wet	20.972	0.69321	4.2983	0.71057	12.214	0.73347
ZTA	Dry	22.664	0.69302	3.9838	0.7102	11.673	0.73314
	Wet	22.679	0.69302	4.3395	0.71034	12.281	0.73325

Table 13. Mechanical Parameters under Static Analysis of Hip Implant at Dry and Wet lubricating condition with the combination of Ti-13Nb-13Zr – Ceramics – UHMWPE – Ti-13Nb-13Zr.

Ceramic		Femoral Head		Liner		Acetabular Cup	
		Stress (MPa)	Deformation (mm)	Stress (MPa)	Deformation (mm)	Stress (MPa)	Deformation (mm)
Alumina	Dry	22.291	0.69303	1.9424	0.71343	12.699	0.73636
	Wet	22.304	0.69303	2.1938	0.71392	13.605	0.73673
Zirconia	Dry	21.013	0.69323	1.9351	0.71367	12.666	0.7366
	Wet	20.978	0.69322	2.1825	0.71416	13.574	0.73697
ZTA	Dry	22.656	0.69303	1.9431	0.71344	12.699	0.73637
	Wet	22.673	0.69302	2.1937	0.71393	13.606	0.73674

Table 14. Mechanical parameters under static analysis of hip implant at dry and wet lubricating condition with the combination of Ni-Ta – Ceramics – HXLPE – Ni-Ta.

Ceramic		Femoral head		Liner		Acetabular cup	
		Stress (MPa)	Deformation (mm)	Stress (MPa)	Deformation (mm)	Stress (MPa)	Deformation (mm)
Alumina	Dry	22.329	0.70137	3.9876	0.71872	11.668	0.74195
	Wet	22.34	0.70137	4.3429	0.71887	12.275	0.74205
Zirconia	Dry	21.004	0.70157	3.9431	0.71895	11.594	0.74217
	Wet	20.976	0.70156	4.3016	0.71911	12.21	0.74228
ZTA	Dry	22.696	0.70137	3.986	0.71873	11.667	11.667
	Wet	22.711	0.70137	4.3427	0.71888	12.276	0.74206

Table 15. Mechanical parameters under static analysis of hip implant at dry and wet lubricating condition with the combination of Ni-Ta – Ceramics – UHMWPE – Ni-Ta.

Ceramic		Femoral head		Liner		Acetabular cup	
		Stress (MPa)	Deformation (mm)	Stress (MPa)	Deformation (mm)	Stress (MPa)	Deformation (mm)
Alumina	Dry	22.321	0.70138	1.9434	0.72197	12.696	0.74517
	Wet	22.334	0.70137	2.1947	0.72245	13.603	0.74554
Zirconia	Dry	21.018	0.70158	1.9364	0.72221	12.663	0.74541
	Wet	20.983	0.70157	2.1835	0.7227	13.572	0.74578
ZTA	Dry	22.689	0.70138	1.9439	0.72198	12.696	0.74518
	Wet	22.706	0.70137	2.1947	0.72246	13.604	0.74555

Table 16. Mechanical parameters under static analysis of hip implant at dry and wet lubricating condition with the combination of Ti-15Mo-5Zr-3Al – Ceramics – HXLPE – Ti-15Mo-5Zr-3Al.

Ceramic		Femoral head		Liner		Acetabular cup	
		Stress (MPa)	Deformation (mm)	Stress (MPa)	Deformation (mm)	Stress (MPa)	Deformation (mm)
Alumina	Dry	22.359	0.70993	3.9899	0.72747	11.663	0.75097
	Wet	22.37	0.70992	4.3462	0.72761	12.271	0.75108
Zirconia	Dry	21.008	0.71012	3.9455	0.7277	11.589	0.7512
	Wet	20.981	0.71011	4.3051	0.72785	12.205	0.75131
ZTA	Dry	22.729	0.70992	3.9882	0.72748	11.661	0.75098
	Wet	22.744	0.70992	4.3459	0.72762	12.272	0.75109

Table 17. Mechanical parameters under static analysis of hip implant at dry and wet lubricating condition with the combination of Ti-15Mo-5Zr-3Al – Ceramics – UHMWPE – Ti-15Mo-5Zr-3Al.

Ceramic		Femoral head		Liner		Acetabular cup	
		Stress (MPa)	Deformation (mm)	Stress (MPa)	Deformation (mm)	Stress (MPa)	Deformation (mm)
Alumina	Dry	22.35	0.70993	1.9443	0.73071	12.693	0.7542
	Wet	22.364	0.70993	2.1957	0.73119	13.601	0.75457
Zirconia	Dry	21.022	0.71014	1.9374	0.73095	12.66	0.75444
	Wet	20.987	0.71012	2.1845	0.73144	13.57	0.75481
ZTA	Dry	22.721	0.70993	1.9449	0.73072	12.694	0.75421
	Wet	22.739	0.70992	2.1957	0.7312	13.602	0.75458

Table 18. Mechanical Parameters under Static Analysis of Hip Implant at Dry and Wet lubricating condition with the combination of Ti-15Mo-5Zr – Ceramics – HXLPE – Ti-15Mo-5Zr.

Ceramic		Femoral head		Liner		Acetabular cup	
		Stress (MPa)	Deformation (mm)	Stress (MPa)	Deformation (mm)	Stress (MPa)	Deformation (mm)
Alumina	Dry	22.69	0.74308	3.9952	0.76136	11.619	0.78597
	Wet	22.706	0.74308	4.3547	0.76151	12.235	0.78607
Zirconia	Dry	21.505	0.74328	3.9512	0.7616	11.549	0.7862
	Wet	21.481	0.74328	4.3141	0.76176	12.174	0.78631
ZTA	Dry	23.236	0.74308	3.9934	0.76137	11.618	0.78598
	Wet	23.255	0.74308	4.3544	0.76152	12.236	0.78609

Table 19. Mechanical parameters under static analysis of hip implant at dry and wet lubricating condition with the combination of Ti-15Mo-5Zr – Ceramics – HXLPE – Ti-15Mo-5Zr.

Ceramic		Femoral head		Liner		Acetabular cup	
		Stress (MPa)	Deformation (mm)	Stress (MPa)	Deformation (mm)	Stress (MPa)	Deformation (mm)
Alumina	Dry	22.683	0.74309	1.9463	0.7646	12.626	0.78919
	Wet	22.701	0.74308	2.1979	0.76508	13.555	0.78956
Zirconia	Dry	21.519	0.7433	1.9397	0.76484	12.594	0.78943
	Wet	21.488	0.74329	2.1867	0.76533	13.526	0.78981
ZTA	Dry	23.228	0.74308	1.9469	0.7646	12.626	0.78919
	Wet	23.25	0.74308	2.1978	0.76509	13.556	0.78957

DISCUSSION

General Findings

The present work is the first of its kind, which develops a fully functioning three-dimensional finite element model of the hip implant and attempts to predict the mechanical performance under varying material and lubricating system. Femoral stem, femoral head, liner and acetabular cup have slightly different movements and functions. Most of the studies [46-47] has focused largely on femoral stem and head with two key interfaces i.e. stem-head and head-liner. The present investigation has been conducted to analyze the frictional behavior of the CoP implant prosthesis. Ceramics are the best-suited materials for femoral head because of high compressive strength, no toxic effects with metal and high wear resistivity.

Current work is focused on the effect of COF for the contact region between liner and head while considering relative motion with femoral stem and acetabular cup. The result of the numerical computation at 2.3 kN loading over the implant assembly shows that the maximum stress is transferred to femoral head and the maximum deformation is observed in the acetabular cup. CoCrMo material with UHMWPE and HXLPE liner demonstrates minimum von-mises stress and deformation as compared to other material combinations, and from three available ceramic materials, Zirconia offers better results as compared to alumina and ZTA ceramics. It has been observed that there is no significant difference between the mechanical parameters obtained from HXLPE and UHMWPE. Since the wear rate of HXLPE is 80% less than alumina, hence HXLPE is the preferred material.

Combination Versus Standard Material

Present finding uses a linear static load of 2.3kN, which is approximately three to four-times the bodyweight of a healthy person. Higher stiff material demonstrates less deformation and provides better mechanical stability. Dry friction causes the polyethylene debris from the liner [48] which causes harmful effects on the human body and leads to implant loosening and failure of an endoprosthesis.

Table 20. Mechanical parameters under static analysis of hip implant at dry and wet lubricating condition with the combination of Ceramics – HXLPE – Ti-6Al-7Nb.

Ceramic		Femoral head		Liner		Acetabular cup	
		Stress (MPa)	Deformation (mm)	Stress (MPa)	Deformation (mm)	Stress (MPa)	Deformation (mm)
Alumina	Dry	28.241	2.4126e-004	3.921	6.2184e-003	11.784	6.4255e-003
	Wet	28.701	2.4451e-004	4.2582	6.6046e-003	12.387	6.6856e-003
Zirconia	Dry	27.751	8.4591e-004	3.8698	6.7174e-003	11.714	6.9166e-003
	Wet	28.22	8.5959e-004	4.2119	7.1235e-003	12.328	7.1924e-003
ZTA	Dry	28.928	2.7535e-004	3.9188	6.2532e-003	11.782	6.4624e-003
	Wet	29.314	2.8112e-004	4.2577	6.6428e-003	12.388	6.7257e-003

Table 21. Mechanical parameters under static analysis of hip implant at dry and wet lubricating condition with the combination of Ceramics – UHMWPE – Ti-6Al-7Nb.

Ceramic		Femoral head		Liner		Acetabular cup	
		Stress (MPa)	Deformation (mm)	Stress (MPa)	Deformation (mm)	Stress (MPa)	Deformation (mm)
Alumina	Dry	28.339	2.4479e-004	1.8208	1.6949e-002	12.53	1.6045e-002
	Wet	28.918	2.4775e-004	2.1071	1.8461e-002	13.497	1.7163e-002
Zirconia	Dry	27.91	8.5917e-004	1.8172	1.746e-002	12.497	1.6545e-002
	Wet	28.495	8.7309e-004	2.0942	1.8997e-002	13.468	1.7682e-002
ZTA	Dry	28.958	2.7645e-004	1.8225	1.6985e-002	12.529	1.6082e-002
	Wet	29.449	2.8323e-004	2.1068	1.8499e-002	13.498	1.7202e-002

Present work also utilizes the femoral stem for analysis purposes, which were not used in previous studies. Table 20 and 21 demonstrates the mechanical parameter for femoral head – liner – acetabular cup for dry and wet condition without

considering femoral stem. Results for femoral head of alumina, zirconia and ZTA with HXLPE liner and Ti-6Al-7Nb cup are tabulated in Table 20, while for UHMWPE is tabulated in Table 21.

The effects of femoral stem consideration on mechanical parameters have been demonstrated in Table 6 and 7. Comparative analysis of results in Table 6 and 20 or Table 7 and 21 clearly distinguishes that stress on femoral head increases (see Table 20), on the other hand, the values of stress for liner and acetabular cup remain relatively similar to results shown in Table 6.

Validation to Prior Studies

No other prior studies have examined the mechanical characteristics under dry and wet lubricating conditions with such a wide range of material combinations. A prior study examinates the femoral stem under 2.3 kN loading. The obtained simulated results using Charnley's model are validated with the available literature data [44] as illustrated in Table 22. It has been analyzed that the present model gives satisfactory outcomes when validated against the published data. The stress, deformation and strains for Ti-6Al-4V and CoCr alloys comes within the error limit of (7.12%, 8.29%), (1.19%, 0.062% and (19.47%, 20.32%) respectively. Table 22 demonstrates the mechanical performance of the implant under patient-specific loadings. Therefore, the findings of the current model simulation are precise and accurate with the available literature.

Table 22. Validation of present work with Chethan et al. [44].

Material (s)		Present work	Chethan et al.	Percentage error
Ti-6Al-4V	Von Mises stress (MPa)	709.64	662.45	7.12 %
	Deformation (mm)	0.45639	0.451	1.19 %
	Strain (mm/mm)	0.0069297	0.0058	19.47 %
CoCr Alloy	Von Mises stress (MPa)	722.7	668.35	8.29 %
	Deformation (mm)	0.25684	0.257	0.0622 %
	Strain (mm/mm)	0.0039707	0.0033	20.32 %

Clinical Implantation

The above-mentioned materials are biocompatible and have the potential to reduce the stress shielding effect by increasing load transfer to the next part and lastly to bone. The current data shows the stress in CoCrMo stem material combination which is less than the Ti alloy implants (see Table 4 to 5). Charnley's hip implant design is clinically proven and largely used as a standard implant for new or revision surgery. Modification in geometries of the implant permits its extensive use for a variety of patients. Geometry of an implant with a multiple size femoral head can be easily accessible with the modification by the simple geometric technique [44]. Chaudhary et al. demonstrated that the COF of the 28 mm femoral head diameter prosthesis is significantly higher than the 36 mm diameter prosthesis for every test repetition. Interestingly, COF for ceramic on ceramic (CoC) with similar geometric combinations for 38 to 36 mm diameter femoral head demonstrates a similar trend of COF [48]. Instrumental study of the hip implant can be carried out by using vibration and acoustic emission (AE) measurement[67]

Novel Contributions

As stated earlier, multiple studies have been performed for an implant but all of them were limited to two or three commonly used materials for stem and femoral head in the implant [49-50]. Therefore, a new study needs to be proposed to analyze the mechanical characteristics of different material-combinations for the stem-head-liner-acetabular cup assembly. Despite of some limitations in our present work, there are notable novel contributions. This work simulates the large combinations of the metals, ceramics and polymers, and used different friction conditions for the static loading of 2.3 kN. The study of mechanical parameters i.e. stress and deformation for three different femoral head material with two different liner materials are first of its kind. Same identical boundary conditions are applicable only for femoral stem which is compared with the available literature data for Ti-6Al-4V and CoCr alloys.

Limitations

Drawbacks/limitations in these types of investigations are common and there is always a scope for future work. Firstly, only a linear axial compressive load is applied over the finite element model of the hip implant [51-52]. The human femur is subjected to the dynamic forces and movements while doing various activities throughout the day like standing, stairs, sitting, walking and climbing [53-54]. Multiple studies demonstrate that the contact force during normal walking ranges between 240-480 % of the body weight (BW). In the present work, the effects of surrounding muscle and tissue have been neglected while applying the ASTM boundary conditions. Since all the chosen materials are biocompatible but after implantation in vivo, implant reaction with the surrounding body fluids and implant degradation are tough to study through software.

Wear between head and liner is not considered in the present work. The effect of two frictional conditions i.e. wet and dry, for a healthy and old aged person is considered. Smoothness or roughness has occurred between the contact region of femoral head and liner. Since the considered materials are metal, ceramics and plastics, therefore implant demonstrates linear isotropic properties, which significantly reduces the computational time. Nonlinear and anisotropic properties influence the bulk behavior of the implant [55]. The manufacturing process of ceramic femoral heads is quite complicated and costlier too, now disruptive by additive manufacturing of advanced ceramics [80-81].

The present research was performed under a constant compression load of 2.3kN, which is approximately three to four times body weight of a 70 kg person. Typical daily activities consist of cyclic loading, while some activities like stumbling and going upstairs produce forces five to six times of body weight. Cyclic loading generates repeated stress, which ultimately leads to fatigue failure of an implant and changes stiffness over time [56]. The main intention of this study is to provide a comparison for the optimum material combination, suited for implantation in vivo and prepares a strong base for future studies. It is expected that the performance of material in the present analysis with multiple combinations would be similar for the real-world clinical scenario for the axial cyclic force during daily life activities.

All the materials which are used in the present work are clinically tested. Every implant design undergoes at least 15-20 years of trials in order to check their compatibility with bone tissues. Present work would be beneficial for future studies because it provides a more clinically relevant scenario. It is very important to know the mechanical behavior of an implant and clinical testing of all the material combinations before implantation into the human body.

Future Scope

Present work demonstrates the effect of dry and wet lubrication conditions with implant under static constraints. The future work leads to continue research with patient anatomic bone assembly under patient specific loading and dynamic constraints. The prediction of fatigue life to calculate the longevity of implant life will be the major topic for future prospective. The inflammation and prediction of wear between femoral head and liner is also an important area to work.

In material prospective, Heterogeneous material distribution is the future of mechanical designs where different objects can be fabricated using various algorithms and computer aided design technique. In Hip Implant design, implant loosening is coming out as a major challenge which needs to be addressed with the help of recent advancements in heterogeneous modeling. The analysis of hip joint can be further explored with heterogeneous material modeling in order to improve the performance and efficiency of the implants design[57-62]. Three-dimensional (3D) printing have significant potential as a fabrication technique as it is capable of biomimicking the anatomical designs found[63].

CONCLUSION

The present investigation consists of two major parts i.e. effect of dry and wet lubricating conditions with three ceramics combinations for UHMWPE and HXLPE liner material. The main conclusions from the present work are as follows:

i. It is found that material combination named CoCrMo – Ceramics – HXLPE – CoCrMo demonstrates the least amount of stress and deformation while Ti-15Mo-5Zr – Ceramics – HXLPE – Ti-15Mo-5Zr shows the highest stresses and deformation.
ii. The highest amount of stress is observed in the order: femoral head > acetabular cup > liner.
iii. Maximum deformation is observed in the order: acetabular cup > liner > femoral head.
iv. It is found that Zirconia ceramic material demonstrates the least amount of stress as compared to Alumina and ZTA.
v. It is found that UHMWPE as a liner material demonstrates less stress but higher deformation than HXLPE plastic.
vi. Dry lubricating condition demonstrates higher stress for femoral head and acetabular cup. But, for liner wet lubricating condition demonstrates higher stress due to lubricating fluid film.
vii. Deformation for the dry and wet lubricating condition is approximately similar for almost every material combination.
viii. The obtained simulated outcomes show that the maximum values of stress-strain for liner and acetabular cup are observed at the center and then continue to reduce towards the outer radius. Additionally, the maximum stress also occurs at the medial side of liner and cup.
ix. It is found that stress-strain for femoral head occurs at the neck contact region. However, maximum deformation is observed on top of the medial side of the head.
x. It is found that interior side of liner and acetabular cup under wet lubricating condition demonstrates maximum stress, strain and deformation. However, the exterior side of liner and interior side of acetabular cup demonstrates similar values of stress and deformation.

Clinical and experimental result demonstrates that HXLPE demonstrates 80% less wear than UHMWPE. Since HXLPE is the next generation material hence it is preferred over UHMWPE. Similarly, ZTA is an advanced material, which overcomes the drawbacks of Alumina and Zirconia. The present work demonstrates that there is no significant difference in the deformation value of Ceramic materials. Finally, the obtained simulated outcomes recommend that implant alloys with ZTA and HXLPE are preferred material-combination as compared to other possible combinations.

ACKNOWLEDGEMENT

The author is grateful to department of mechanical engineering of NIT Kurukshetra and co-authors for their endless contribution and supervision.

REFERENCES

[1] S. Affatato, N. Freccero, and P. Taddei, “The biomaterials challenge: A comparison of polyethylene wear using a hip joint simulator,” *J. Mech. Behav. Biomed. Mater*., vol. 53, pp. 40-48, 2016, doi: 10.1016/j.jmbbm.2015.08.001.

[2] M. Merola, and S. Affatato, "Materials for hip prostheses: a review of wear and loading considerations," *Materials.*, vol. 12, no. 3, 2019, 495, doi: 10.3390/ma12030495.

[3] S. Kurtz, K. Ong, E. Lau, F. Mowat, and M. Halpern, “Projections of primary and revision hip and knee arthroplasty in the United States from 2005 to 2030,” *J. Bone Jt. Surg*., vol. 89, no. 4, pp. 780–785, 2007, doi: 10.2106/JBJS.F.00222.

[4] S. Affatato, A. Ruggiero, and M. Merola, “Advanced biomaterials in hip joint arthroplasty. A review on polymer and ceramics composites as alternative bearings,” *Compos. Part B: Engg*., vol. 83, pp. 276–283, 2015, doi: 10.1016/j.compositesb.2015.07.019.

[5] L. Mattei, F. D. Puccio, E. Ciulli, and A. Pauschitz, "Experimental investigation on wear map evolution of ceramic-on-UHMWPE hip prosthesis," *Tribol. Int.*, vol. 143, no. 106068, 2020, doi: 10.1016/j.triboint.2019.106068.

[6] M.J. Lysaght, and J.A. O'Loughlin, “Demographic scope and economic magnitude of contemporary organ replacement therapies,” *ASAIO J*., vol. 46, no. 5, pp. 515–521, 2000, doi: 10.1097/00002480-200009000-00001.

[7] A. L. Neuwirth, B. S. Ashley, W. M. Hardaker, and N. P. Sheth, "Metal-on-metal hip implants: progress and problems," *In Biomedical Applications of Metals*., pp. 73-93, Springer, Cham, 2018, doi: 10.1007/978-3-319-74814-6_3.

[8] L.I. Havelin *et al.*, “The Nordic Arthroplasty Register Association: a unique collaboration between 3 national hip arthroplasty registries with 280, 201 THRs,” *Acta orthopaedica.*, vol. 80, no. 4, pp. 393–401, 2009, doi: 10.3109/17453670903039544.

[9] D. R. Bijukumar *et al.*, "Systemic and local toxicity of metal debris released from hip prostheses: A review of experimental approaches," *Nanomed.: Nanotechnol. Biol. Med.*, vol. 14, no. 3, pp. 951-963, 2018, doi: 10.1016/j.nano.2018.01.001.

[10] K. Huch *et al.*, “Sports activities 5 years after total knee or hip arthroplasty: the Ulm Osteoarthritis Study,” *Ann. Rheum. Dis..*, vol. 64, no. 12, pp. 1715–1720, 2005, doi: 10.1136/ard.2004.033266.

[11] C. A. Myers *et al.*, "The impact of hip implant alignment on muscle and joint loading during dynamic activities," *Clin. Biomech..*, vol. 53, pp. 93-100, 2018, doi: 10.1016/j.clinbiomech.2018.02.010.

[12] G. B. Flugsrud *et al.*, “The effect of middle-age body weight and physical activity on the risk of early revision hip arthroplasty,” *Acta Orthopaedica.*, vol. 78, no.1, pp. 99–107, 2007, doi: 10.1080/17453670610013493.

[13] H. Malchau, P. Herberts, and L. Ahnfelt, “Prognosis of total hip replacement in Sweden: follow-up of 92,675 operations performed 1978–1990,” *Acta Orthopaedica Scandinavica.*, vol. *64*, no. 5, pp. 497-506, doi: 10.3109/17453679308993679.

[14] S. Mayor, "Registry data show increase in joint replacement surgery," no. 358, 2017, doi: 10.1136/bmj.j4324.

[15] A. Rahman *et al.*, “In vivo and in vitro outcomes of alumina, zirconia and their composited ceramic-on-ceramic hip joints,” *J. Ceram. Soc.*, vol. 121, no. 1412, pp. 382-387, 2013, doi: 10.2109/jcersj2.121.382.

[16] R. E. Kennon *et al.*, Total hip arthroplasty through a minimally invasive anterior surgical approach," *JBJS.,* vol. 85, no. suppl_4, pp. 39-48, 2003, doi:10.2106/00004623-200300004-00005.

[17] S. Ghosh, D. Choudhury, N. S. Das, and B. P. Murphy, “Tribological role of synovial fluid compositions on artificial joints—a systematic review of the last 10 years,” *Lubr. Sci..*, vol. 26, no. 6, pp. 387-410, 2014, doi: 10.1002/ls.1266.

[18] S. A. Jaber, and S. Affatato,"An overview of in vitro mechanical and structural characterization of hip prosthesis components," *Biomaterials in Clinical Practice.*, pp. 585-599, 2018, doi: 10.1007/978-3-319-68025-5_22.

[19] M. J. Nine *et al.*, “Wear debris characterization and corresponding biological response: artificial hip and knee joints,” *Materials.*, vol. 7, no. 2, pp. 980–1016, 2014, doi: 10.3390/ma7020980.

[20] E. Jämsen *et al.*, "Characterization of macrophage polarizing cytokines in the aseptic loosening of total hip replacements." *J. Orthop. Res..*, vol. 32, no. 9, pp. 1241-1246, 2014, doi: 10.1002/jor.22658.

[21] F. D. Puccio, and L. Mattei, “Biotribology of artificial hip joints,” *World J. Orthop.*, vol. 6, no. 1, pp. 77-94, 2015, doi: 10.5312/wjo.v6.i1.77.

[22] Z. R. Zhou, and Z. M. Jin, “Biotribology: recent progresses and future perspectives,” *Biosurf. Biotribol.*, vol. 1, no. 1, pp. 3-24, 2015, doi: 10.1016/j.bsbt.2015.03.001.

[23] S. C. Scholes, A. Unsworth, R. M. Hall, and R. Scott, “The effects of material combination and lubricant on the friction of total hip prostheses,” *Wear.*, vol. 241, no. 2, pp. 209-213, 2000, doi:10.1016/S0043-1648(00)00377-X.

[24] M. Merola, and S. Affatato, “Materials for hip prostheses: A review of wear and loading considerations,” *Materials.*, vol. 12, no. 3, pp. 495, 2019, doi:10.3390/ma12030495.

[25] Y. Wang, S. Arabnejad, M. Tanzer, and D. Pasini, "Hip implant design with three-dimensional porous architecture of optimized graded density," *J. Mech. Des.*, vol. 140, no. 11, 2018, 111406, doi: 10.1115/1.4041208.

[26] D. Dowson, C. Hardaker, M. Flett, and G. H. Isaac, “A hip joint simulator study of the performance of metal-on-metal joints: Part II: design,” *J. Arthroplasty.*, vol. 19, no. 8, pp. 124-130, 2004, doi. 10.1016/j.arth.2004.09.016.

[27] C. R. Bragdon *et al.*, “Radiostereometric analysis comparison of wear of highly cross-linked polyethylene against 36-vs 28-mm femoral heads,” *J. Arthroplasty.*, vol. 22, no. 6, pp. 125-129, 2007, doi: 10.1016/j.arth.2007.03.009.

[28] R. M. Hall, and A. Unsworth, “Friction in hip prostheses,” *Biomaterials.*, vol. 18, no. 15, pp. 1017-1026, 1997, doi: 10.1016/S0142-9612(97)00034-3.

[29] D. Xiong, and S. Ge, “Friction and wear properties of UHMWPE/Al2O3 ceramic under different lubricating conditions,” *Wear.*, vol. 250, no. 1-12, pp. 242-245, 2001, doi: 10.1016/S0043-1648(01)00647-0.

[30] M. Sobociński, “Analysis of friction and lubrication of human joint's surfaces,” *J. Appl. Comput. Mech.*, vol. 15, no. 1, pp. 161-167, 2016, doi: 10.17512/jamcm.2016.1.16.

[31] J. H. Dumbleton *et al.*, “The basis for a second-generation highly cross-linked UHMWPE,” *Clin. Orthop. Relat. Res.,* vol. 453, pp. 265-271, 2006, doi: 10.1097/01.blo.0000238856.61862.7d.

[32] R.Takada *et al.*, "Comparison of wear rate and osteolysis between second-generation annealed and first-generation remelted highly cross-linked polyethylene in total hip arthroplasty. A case control study at a minimum of five years," *Orthop. Traumatol. Surg. Res.*, vol. 103, no. 4, pp. 537-541, 2017, doi: 10.1016/j.otsr.2017.02.004.

[33] J. A. D’Antonio, W. N. Capello, and R. Ramakrishnan, “Second-generation annealed highly cross-linked polyethylene exhibits low wear,” *Clin. Orthop. Relat. Res.,* vol. 470, no. 6, pp. 1696-1704, 2012, doi: 10.1007/s11999-011-2177-3.

[34] S. E. Reynolds, A. L. Malkani, R. Ramakrishnan, and M. R. Yakkanti, "Wear analysis of first-generation highly cross-linked polyethylene in primary total hip arthroplasty: an average 9-year follow-up," *J. Arthroplasty*, vol. 7, no. 6, pp. 1064-1068, 2012, doi: 10.1016/j.arth.2012.01.006.

[35] M. Geetha, A.K. Singh, R. Asokamani, and A.K. Gogia, "Ti based biomaterials, the ultimate choice for orthopaedic implants – A review," *Prog. Mater. Sci.*., vol. 54, no. 3, pp. 397-425, 2009, doi: 10.1016/j.pmatsci.2008.06.004.

[36] A. T. Şensoy, M. Çolak, I. Kaymaz, and F. Findik, "Optimal material selection for total hip implant: A finite element case study," *Arab. J. Sci. Eng.*, vol. 44, no. 12, pp. 10293-10301, 2019, doi: 10.1007/s13369-019-04088-y.

[37] A. Ruggiero, M. Merola, and S. Affatato, "Finite element simulations of hard-on-soft hip joint prosthesis accounting for dynamic loads calculated from a musculoskeletal model during walking," *Materials.*, vol. 11, no. 4, pp. 574, 2018, doi:10.3390/ma11040574.

[38] R. Sharma, V. K. Mittal, and V. Gupta, "Homogeneous modelling and analysis of hip prosthesis using FEA," *J. Phys. Conf. Ser., IOP Publishing.*, vol. 1240, no. 1, pp. 012118, 2019, doi: 10.1088/1742-6596/1240/1/012118.

[39] T. Joshi, R. Sharma, V. K. Mittal, and V. Gupta, "Comparative investigation and analysis of hip prosthesis for different bio-compatible alloys," *Mat. Tod. Proc.,* Vol. 43, no. 1, pp. 105-111, 2021, doi: 10.1016/j.matpr.2020.11.222.

[40] T. Joshi, and G. Gupta, "Effect of dynamic loading on hip implant using finite element method," *Mat. Tod. Proc.*, 2021, doi: 10.1016/j.matpr.2020.11.378.

[41] R. N. Stauffer, "Ten-year follow-up study of total hip replacement," *J. Bone Jt. Surg. Am*., vol. 64, no. 7, pp. 983–990, 1982.

[42] R. K. Sinha, "Hip replacement: current trends and controversies," CRC press, Taylor & Francis group., Marcel Dekker: New York City, NY, USA, 2002.

[43] Charnley Modular Surgical Technique, Depuy synthes, 2018. [online]. Available: https://www.corailpinnacle.net/sites/default/files/2018-05/DSEMJRC07160668%20CHARNLEY%20Modular%20ST.pdf

[44] K. N. Chethan *et al.*, "Static structural analysis of different stem designs used in total hip arthroplasty using finite element method," *Heliyon.*, vol. 5, no. 6, pp. e01767, 2019, doi:10.1016/j.heliyon.2019.e01767.

[45] H. Bougherara *et al.*, "A preliminary biomechanical study of a novel carbon-fibre hip implant versus standard metallic hip implants," *Med Eng Phys.*, vol. 33, no. 1, pp.121-128, 2011, doi:10.1016/j.medengphy.2010.09.011.

[46] S. Shankar, and R. Nithyaprakash, "Effect of radial clearance on wear and contact pressure of hard-on-hard hip prostheses using finite element concepts," *Tribol. Trans.*, vol. 57, no. 5, pp. 814-820, 2014, doi: 10.1080/10402004.2014.915072.

[47] A. Haringova, K. Stračár, and K. Prikkel, "The experimental verification of effect of lubrication on coefficient of friction in endoprosthesis of hip joint," *Hidraulica.*, vol. 3, p. 7, 2014.

[48] D. Choudhury *et al.*, "The impact of surface and geometry on coefficient of friction of artificial hip joints," *J. Mech. Behav. Biomed. Mater.*, vol. 72, pp. 192-199, 2017, doi:10.1016/j.jmbbm.2017.05.011.

[49] A. T. Şensoy, M. Çolak, I. Kaymaz, and F. Findik, " optimal material selection for total hip implant: a finite element case study," *Arab J Sci Eng.*, vol. 44, no. 12, pp. 10293–10301, 2019, doi:10.1007/s13369-019-04088-y.

[50] P. Damm *et al.*, "Total hip joint prosthesis for in vivo measurement of forces and moments," *Med. Eng. Phys.*, vol. 32, no. 1, 2010, pp. 95-100, doi: 10.1016/j.medengphy.2009.10.003.

[51] G. N. Duda *et al.*, "Influence of muscle forces on femoral strain distribution," *J. Biomech.*, vol. 31, no. 9, pp. 841-846, 1998, doi: 10.1016/S0021-9290(98)00080-3.

[52] M. E. Taylor *et al.*, " Stress and strain distribution within the intact femur: compression or bending," *Med. Eng. Phy.*, vol. 18, no. 2, pp. 122–131, 1996, doi: 10.1016/1350-4533(95)00031-3.

[53] G. Bergmann *et al.*, "Realistic loads for testing hip implants," *Biomed. Mater. Eng.*, vol. 20, no. 2, pp. 65-75, 2010, doi:10.3233/BME-2010-0616.

[54] C. Fabry *et al.*, "Generation of physiological parameter sets for hip joint motions and loads during daily life activities for application in wear simulators of the artificial hip joint," *Med. Eng. Phy.*, vol. 35, no. 1, pp. 131-139, 2013, doi: 10.1016/j.medengphy.2012.07.014.

[55] M. Campbell, M. N. Bureau, and L. H. Yahia, "Performance of CF/PA12 composite femoral stems," *J Mater Sci: Mater Med.*, vol. 19, no. 2, pp. 683–93, 2008, doi: 10.1007/s10856-007-3073-y.

[56] M. Talbot, R. Zdero, and E. H. Schemitsch, "Cyclic loading of periprosthetic fracture fixation constructs," *J Trauma.*, vol. 64, no. 5, pp. 1308–1312, 2008, doi: 10.1097/ta.0b013e31811ea244.

[57] V. Gupta, V. K. Bajpai, and P. Tandon, "Slice generation and data retrieval algorithm for rapid manufacturing of heterogeneous objects," *Comput. Aided Des. Appl.*, vol. 11, no. 3, pp. 255–262, 2014, doi:10.1080/16864360.2014.863483.

[58] V. Gupta and P. Tandon, "Heterogeneous object modeling with material convolution surfaces," *Comput.-Aided Design.*, vol. 62, pp. 236–247, 2015, doi:10.1016/j.cad.2014.12.005.

[59] V. Gupta and P. Tandon, "Heterogeneous composition adaptation with material convolution control features," *ASME. J. Comput. Inf. Sci. Eng.*, vol. 17, no. 2, 2017, doi: 10.1115/1.4034741.

[60] V. Gupta, K. S. Kasana, and P. Tandon, "Reference based geometric modeling for heterogeneous objects," *Comput.-Aided Design Applications.*, vol. 9, no. 2, pp. 155–165, 2012, doi: 10.3722/cadaps.2012.155-165.

[61] V. Gupta and R. Ranjan, "Rapid prototyping of heterogeneous objects: issues and challenges," *Asian Rev. Mech. Eng*., vol. 5, pp. 24–29, 2016.

[62] V. Gupta, K. S. Kasana, and P. Tandon, "Computer aided design modeling for heterogeneous objects," *International Journal of Computer Science Issues.*, vol. 7, no. 2, pp. 31-38, 2010, https://arxiv.org/abs/1004.3571.

[63] O. Obinna, I. Stachurek, B. Kandasubramanian, and J. Njuguna,"3D printing for hip implant applications: A review," *Polymers.*, vol. 12, no. 11, 2020, 2682, doi: 10.3390/polym12112682.

[64] P. Bracco, A. Bellare, A. Bistolfi, and S. Affatato,"Ultra-high molecular weight polyethylene: influence of the chemical, physical and mechanical properties on the wear behavior. A review," *Materials*., vol. 10, no. 7, 2017, 791, doi: 10.3390/ma10070791.

[65] S. Affatato, S. A. Jaber, and P. Taddei, "Ceramics for hip joint replacement" *In Biomaterials in Clinical Practice*., pp. 167-181. Springer, Cham, 2018, doi: 10.1007/978-3-319-68025-5_7.

[66] M. A. Hajjar *et al.*, "Wear of composite ceramics in mixed-material combinations in total hip replacement under adverse edge loading conditions," *J. Biomed. Mater. Res. B: Appl. Biomater*., vol. 105, no. 6, pp. 1361-1368, 2017, doi: 10.1002/jbm.b.33671.

[67] Y. Qiblawey *et al.*, "Instrumented hip implant: A review." *IEEE Sensors Journal*., vol. 21, no. 6, pp. 7179-7194, 2020, doi: 10.1109/JSEN.2020.3045317.
[68] A. Vulović and N. Filipovic, "Computational analysis of hip implant surfaces," *J. Serb. Soc. Comput. Mech.*, 2019, doi: 10.24874/jsscm.2019.13.01.07.
[69] K. Čolić *et al.*, "Experimental and numerical research of mechanical behaviour of titanium alloy hip implant," *Tehnički vjesnik–Technical Gazette*., vol. 24, no. 3, pp. 709-713, 2017, doi: 10.17559/TV-20160219132016.
[70] K. N. Chethan, N. S. Bhat, M. Zuber, and B. S. Shenoy, "Finite element analysis of hip implant with varying in taper neck lengths under static loading conditions," *Comput. Methods Programs Biomed*., vol. 208, 2021, 106273, doi: 10.1016/j.cmpb.2021.106273.
[71] N. Kladovasilakis, K. Tsongas, and D. Tzetzis, "Finite element analysis of orthopedic hip implant with functionally graded bioinspired lattice structures," *Biomimetics*., vol. 5, no. 3, 2020, 44, doi: 10.3390/biomimetics5030044.
[72] K. M. Abate, A. Nazir, and J. Y. Jeng, "Design, optimization, and selective laser melting of vin tiles cellular structure-based hip implant," *Int. J. Adv. Manuf. Technol*., vol. 112, no. 7, pp. 2037-2050, 2021, doi: 10.1007/s00170-020-06323-5.
[73] D. Royhman *et al.*, "In vitro simulation of fretting-corrosion in hip implant modular junctions: the influence of pH," *Med. Eng. Phys.*, vol. 52, pp. 1-9, 2018, doi: 10.1016/j.medengphy.2017.10.016.
[74] K. N. Chethan, N. S. Bhat, M. Zuber, and B. S. Shenoy, "Finite element analysis of different hip implant designs along with femur under static loading conditions," *J. Biomed. Phys. Eng.*, vol. 9, no. 5, 2019, 507, doi: 10.31661/jbpe.v0i0.1210.
[75] S. Ghosh, S. Abanteriba, S. Wong, and S. Houshyar, "Selective laser melted titanium alloys for hip implant applications: Surface modification with new method of polymer grafting," *J. Mech. Behav. Biomed. Mater.*, vol. 87, pp. 312-324, 2018, doi: 10.1016/j.jmbbm.2018.07.031.
[76] C. Goswami *et al.*, "Fabrication of ceramic hip implant composites: influence of silicon nitride on physical, mechanical and wear properties." *Silicon*., vol. 12, no. 5, pp. 1237-1245, 2020, doi: 10.1007/s12633-019-00222-5.
[77] S. Konan, M. P. Abdel, and F. S. Haddad, "Cemented versus uncemented hip implant fixation: Should there be age thresholds?," *Bone Jt. Res.*, vol. 8, no. 12, pp. 604-607, 2019, doi: 10.1302/2046-3758.812.BJR-2019-0337.
[78] C. Goswami *et al.*, "Physico-mechanical and surface wear assessment of magnesium oxide filled ceramic composites for hip implant application," *Silicon.*, vol. 11, no. 1, pp. 39-49, 2019, doi: 10.1007/s12633-018-9880-6.
[79] C. KN, M. Zuber, S. Bhat N, and S. Shenoy B. "Optimized trapezoidal-shaped hip implant for total hip arthroplasty using finite element analysis," *Cogent Eng.*, vol. 7, no. 1, 2020, 1719575, doi: 10.1080/23311916.2020.1719575.
[80] J. Su *et al.*, "In vitro analysis of wearing of hip joint prostheses composed of different contact materials," *Materials*., vol. 14, no. 14, pp. 3805, 2021, doi:10.3390/ma14143805.
[81] Y. Lakhdar, C. Tuck, J. Binner, A. Terry, and R. Goodridge, "Additive manufacturing of advanced ceramic materials," *Prog. Mater. Sci.*, vol. 116, no. 100736, 2021, doi: 10.1016/j.pmatsci.2020.100736